micro

MDPI

Article

Sacrificial Doping as an Approach to Controlling the Energy Properties of Adsorption Sites in Gas-Sensitive ZnO Nanowires

Svetlana Nalimova [1,*], Zamir Shomakhov [2], Anton Bobkov [1] and Vyacheslav Moshnikov [1]

[1] Department of Micro- and Nanoelectronics, Saint Petersburg Electrotechnical University "LETI", Professor Popov Str. 5, 197022 St. Petersburg, Russia
[2] Department of Electronics and Information Technologies, Kabardino-Balkarian State University Named after H.M. Berbekov, Chernyshevsky Str. 173, 360004 Nalchik, Russia
* Correspondence: sskarpova@list.ru

Abstract: Currently, devices for environmental gas analyses are required in many areas of application. Among such devices, semiconductor-resistive gas sensors differ advantageously. However, their characteristics need further improvement. The development of methods for controlling the surface properties of nanostructured metal oxides for their use as gas sensors is of great interest. In this paper, a method involving the sacrificial doping of ZnO nanowires to control the content of their surface defects (oxygen vacancies) was proposed. Zinc oxide nanowires were synthesized using the hydrothermal method with sodium iodide or bromide as an additional precursor. The surface composition was studied using X-ray photoelectron spectroscopy. The sensor properties of the isopropyl alcohol vapors at 150 °C were studied. It was shown that a higher concentration of oxygen vacancies/hydroxyl groups was observed on the surfaces of the samples synthesized with the addition of iodine and bromine precursors compared to the pure zinc oxide nanowires. It was also found out that these samples were more sensitive to isopropyl alcohol vapors. A model was proposed to explain the appearance of additional oxygen vacancies in the subsurface layer of the zinc oxide nanowires when sodium iodide or sodium bromide was added to the initial solution. The roles of oxygen vacancies and surface hydroxyl groups in providing the samples with an increased sensitivity were explained. Thus, a method involving the sacrificial doping of zinc oxide nanowires has been developed, which led to an improvement in their gas sensor characteristics due to an increase in the concentration of oxygen vacancies on their surface. The results are promising for percolation gas sensors equipped with additional water vapor traps that work stably in a high humidity.

Keywords: zinc oxide; gas sensor; nanowires; X-ray photoelectron spectroscopy; sacrificial doping; defects; oxygen vacancies

Citation: Nalimova, S.; Shomakhov, Z.; Bobkov, A.; Moshnikov, V. Sacrificial Doping as an Approach to Controlling the Energy Properties of Adsorption Sites in Gas-Sensitive ZnO Nanowires. *Micro* **2023**, *3*, 591–601. https://doi.org/10.3390/micro3020040

Academic Editors: Rosaria A. Puglisi, Jost Adam and Ray Duffy

Received: 27 February 2023
Revised: 8 May 2023
Accepted: 23 May 2023
Published: 1 June 2023

1. Introduction

Gas sensors are of great interest indifferent application areas, such as environmental monitoring, biomedical devices, and the pharmaceutical industry, etc. Common gas-sensitive materials include polymers [1], semiconductor materials based on metal oxides [2,3], and porous silicon [4,5], etc. The characteristics of gas sensors are sensitivity, a detection limit, response time, recovery time, selectivity, operating temperature, resolution, and stability.

Sensors based on nanostructured metal oxides have many advantages, such as a low cost, the possibility of an environmentally friendly synthesis, and a high sensitivity [6,7]. Different approaches can be used to improve the sensitivity and selectivity of metal oxides [8]. The most advantageous way to do this is to develop new nanomaterials and new methods for the synthesis of nanostructured active layers. This includes the formation of heterostructures to improve the catalytic activity and adsorption capacity [9] and an improvement in the characteristics of the sensor using an atomic-molecular design and the control of the surface defect structure [10,11].

Zinc oxide is widely used as a gas-sensitive material [12–14]. It is a wide-bandgap n-type semiconductor with advantages such as biocompatibility, chemical stability, environmental safety, and a low cost. Zinc oxide nanostructures of different sizes and shapes can be synthesized, for example, into nanoparticles, one-dimensional (1D), two-dimensional (2D), and three-dimensional (3D) structures [15]. Different doping approaches for improving their gas sensitivity have been developed, for example, doping with metal elements, hetero-atomic doping, and co-doping [16]. The design of composites based on zinc oxide is also a promising way to achieve a high sensitivity [17].

An important factor in achieving enhanced sensor properties is the presence of point defects [18,19], mainly oxygen vacancies, on the surface of the gas-sensitive layer, which are adsorption sites for oxidizing gases, in particular oxygen [20]. For example, in [21], it was shown that oxygen vacancies affected the oxygen absorption on the surface of WO_{3-x} nanostructures and facilitated the adsorption of negatively charged oxygen ions, leading to an improvement in the sensor characteristics and a decrease in the operating temperature. Negatively charged chemisorbed oxygen ions take part in chemical reactions and the formation of sensor signals. The content of the oxygen vacancies in zinc oxide can be increased mechanically, as well as during synthesis or post-treatment in a reducing or oxygen-deficient atmosphere, in both the gas and liquid phases, using special precursors [22].

Sensors with percolation structures have been developed to increase sensitivity [23]. In such sensors, the current flows through nanowires localized on the substrate surface using nanolithography techniques. The nanowires located separately are not connected with the conducting channels and can perform other functions, for example, adsorb water vapor. It is known that the cross-adsorption of water vapor on the sensor layer surface leads to a degradation of the sensor characteristics. Thus, a crucial issue is the development methods for modifying the hydrophilic properties the nanowires' surfaces, including sacrificial doping.

Recently, X-ray photoelectron spectroscopy (XPS) has been widely used in material chemistry and physics to assess surface chemistry, the features of chemical bonding, and the compositions of surface layers and phase boundaries. XPS is based on the effect of the chemical environment of an atom on the binding energy of electrons (chemical shift). Thus, the structure of chemical bonds and their changes depending on the synthesis conditions or post-treatment can be revealed. Due to its high accuracy, XPS is suitable for studying the defect states on the surfaces of materials. It has been shown that, with an increase in the annealing temperature, the content of oxygen vacancies increases on the surface of a thin zinc oxide film [24]. The redistribution of surface active sites at the formation of $ZnFe_2O_4$ and $ZnSnO_3$, as well as the dependence of their sensor and structural properties on the surface functional composition, were studied in [25–27]. It was found that the adsorption properties of metal oxides depend on their surface contents of hydroxyl groups, ionosorbed oxygen, and defect states, especially vacancies in O sublattice [23].

In this paper, a method for designing defect structures on the surfaces of atomic and molecular structures is proposed for the first time. The issues of a defect structure analysis and its influence on the sensor properties of metal oxide nanostructures are studied. Defect design methods may include adding sacrificial dopants at the formation of atomic-molecular oxide layers, with a subsequent modification of the surface layers. This work is aimed at the development of sacrificial doping techniques for the controlled formation of defect surface structures on zinc oxide nanowires, the analysis of changes in the surface's chemical composition as a result of this doping, and the effect of the defect structure on the sensor properties of the zinc oxide nanowires.

2. Materials and Methods

To synthesize the gas-sensitive layers, the following raw materials of a high-purity grade were used: zinc acetate, hexamethylenetetramine, zinc nitrate hexahydrate, sodium iodide, and sodium bromide (LenReactiv, Russia). A sensor platform with gold interdigitated electrodes (BI2, Tesla Blatna, Czech Republic) was used as a substrate.

The zinc oxide nanowires' layers were produced using hydrothermal synthesis. Initially, seeds of zinc oxide nanoparticles were synthesized on a sensor platform with aspin-coating of an aqueous solution of zinc acetate (5 mM) and annealed at 350 °C. The zinc oxide nanowires were formed on the seed layers. The hydrothermal synthesis was carried out in an equimolar (100 mM) aqueous solution of hexamethylenetetramine ($C_6H_{12}N_4$) and zinc nitrate hexahydrate ($Zn(NO_3)_2 \cdot 6H_2O$). The iodine- and bromine-doped samples were synthesized with an addition of sodium iodide or sodium bromide (10 mM) to the solution, respectively. The ZnO nanowires layers were grown for one hour at 86 °C. The following step was the annealing at 350 °C for 30 min. The scheme of the sensor is shown in Figure 1.

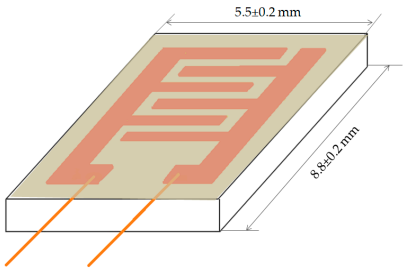

Figure 1. Schematic of the sensor based on zinc oxide nanowire layer.

The surface morphology was studied using scanning electron microscopy, SEM (Zeiss Supra25, Carl Zeiss, Germany).

The surface chemical composition of the layers consisting of the ZnO nanowires was investigated via X-ray photoelectron spectroscopy using the Thermo Scientific X-ray photoelectron spectrometer K-Alpha (USA). Monochromatic Al-Ka radiation (hν = 1486.7 eV) was used to excite the photoemission. Survey spectra were obtained in the range of the binding energies from 0 to 1350 eV. The spectra of the elements with a width of 20 eV were taken in order to more accurately identify the position of the peaks. The decomposition of the core-level spectra was carried out to determine the contents of the elements in different bound states.

The sensor properties were analyzed when the sample was exposed to vapors of isopropyl alcohol with a concentration of 1000 ppm at 150 °C. This temperature was chosen because of the peculiarities of the oxygen chemisorption on the zinc oxide surfaces. The maximum response was observed in the temperature range of 300–400 °C. However, such temperatures restrict the practical application of the sensors, limiting their integration with portable devices. Therefore, the study of these sensor properties at lower temperatures is of interest. The sample was placed in a chamber alternately purged with dried air and a mixture of air with isopropyl alcohol vapors (Figure 2). The sample was fixed on the heating element inside the chamber with clamping contacts. The isopropyl alcohol vapor concentration was set with rotameters by mixing the diluent air stream and isopropyl alcohol vapor stream obtained by passing the air stream through a bubbler tank. The air mixture with the isopropyl alcohol vapor was supplied to the sample surface. The final concentration of isopropyl alcohol was obtained by:

$$C = \frac{P_{gas} F_{gas}}{P_{atm}(F_{gas} + F_{air})},$$

where P_{gas} is the saturation vapor pressure of the bubbled fluid, F_{gas} is the air flow rate through the bubbler tank, P_{atm} is the atmospheric pressure (taken as 760 mm Hg), and F_{air} is the diluent air flow rate. The saturation vapor pressure was calculated using the Antoine equation:

$$P_{gas} = 10^{A - \frac{B}{C+T}},$$

where A, B, and C are the approximation table parameters and T is the fluid temperature. The current was measured using a KEITHLEY 6485 picoammeter. The bias voltage was 5 V. The sensitivity of the sample (S) was calculated as:

$$S = \frac{R_{air}}{R_{gas}},$$

where R_{air} is the resistance of the sample in the air and R_{gas} is the resistance of the sample in the presence of the target gas.

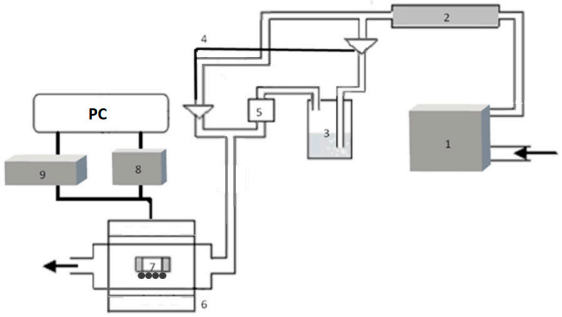

Figure 2. Schematic of gas-sensing measuring setup: 1—compressor, 2—dehumidifier, 3—bubbler tank, 4—rotameters, 5—electromechanical valve, 6—chamber, 7—sample, 8—controller, and 9—measuring equipment.

3. Results

Figure 3 shows the typical microstructure of a zinc oxide nanowire layer synthesized under the conditions described above. It was found that the diameter of the nanowires was 20–120 nm and the average length was about 200 nm.

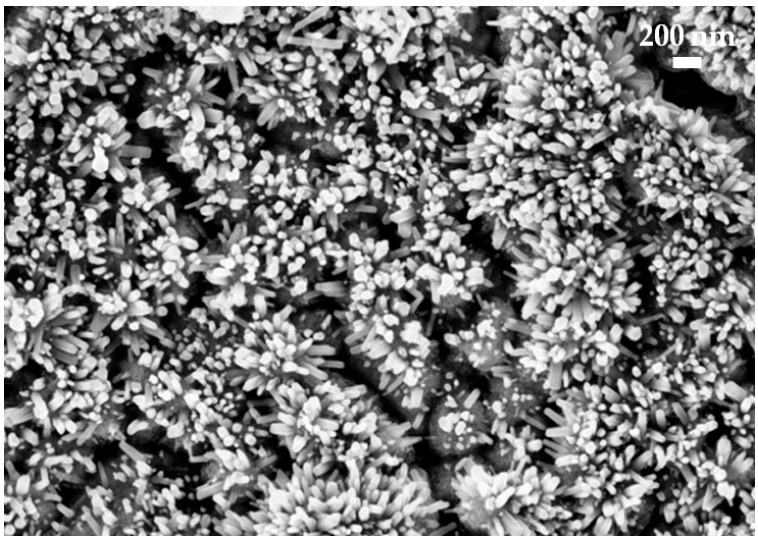

Figure 3. SEM image of zinc oxide nanowire layer.

Peaks corresponding to zinc, oxygen, and carbon were observed on the survey spectra of the pure and doped ZnO nanowires (Figure 4). The positions of these peaks matched with the results reported by other authors [28]. The presence of carbon peaks on the surface of the samples was attributed to the adsorption of hydrocarbons from the environment [29].

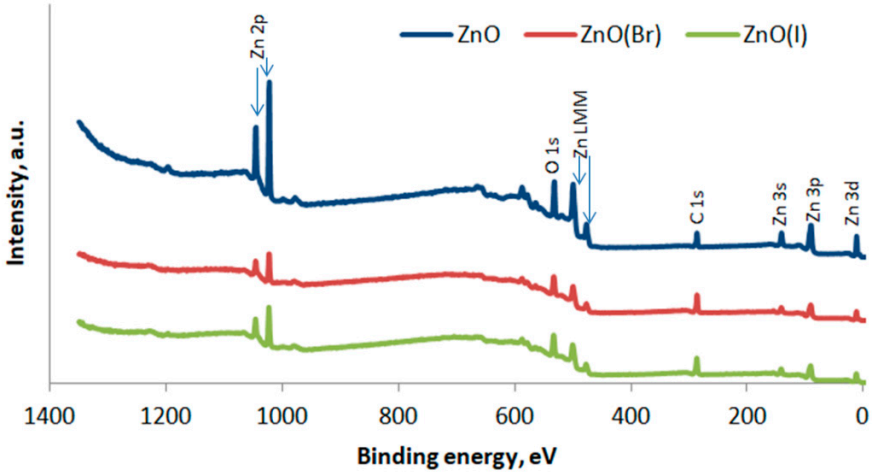

Figure 4. Survey XPS spectra of zinc oxide nanowires.

The spectra of the Zn2p levels (Figure 5) consisted of $Zn2p_{3/2}$ and $Zn2p_{1/2}$ peaks with maximums at 1021.3 eV and 1044.4 eV, correspondingly. The binding energies corresponded to the Zn^{2+} atoms (Zn–O) in a zinc oxide crystal lattice. The difference between the peak positions was ~23.1 eV, which agreed well with the spin-orbit splitting of the Zn2p level in zinc oxide [30].

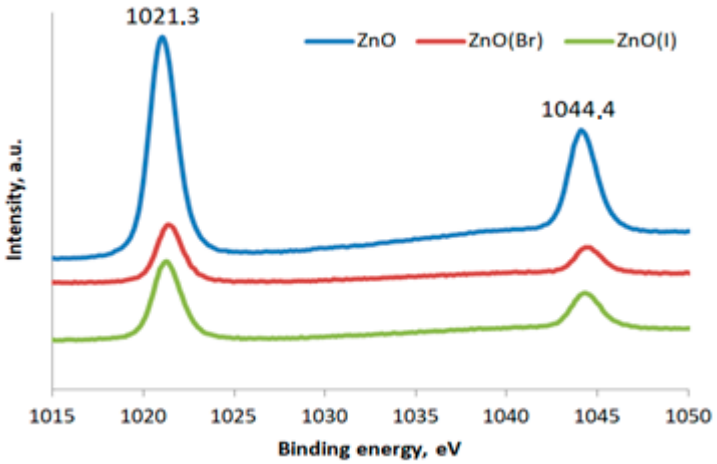

Figure 5. XPS spectra of Zn2p levels.

Figure 6 shows the spectra of the O1s levels of all the samples. The spectra exhibit asymmetry, which can be attributed to the several types of oxygen bonds in the zinc oxide subsurface area. The spectra can be deconvoluted into at least two peaks. This deconvolution was performed by using the Gauss fitting. Table 1 shows the position, FWHM, and relative contributions of the component peaks. The O_{lat} peaks at 529.8 eV for ZnO and 530.1 eV for ZnO(I) and ZnO(Br) corresponded to the O^{2-} ions in a zinc oxide lattice [31]. The O_{vac} components, with higher binding energies of 531.3 eV for ZnO and ~531.8 eV for ZnO(I) and ZnO(Br), corresponded to O^{2-} ions with a lower valence electron density and could be ascribed to hydroxyls bonds, i.e., HO–ZnO, or O^{2-} ions in the oxygen-deficient regions of a zinc oxide crystal lattice [32]. It was found that the addition of precursors for the sacrificial doping to the growth solution resulted in a significant increase in the oxygen contents corresponding to the oxygen vacancies or surface hydroxyl groups. It was also found that, for the samples synthesized with an addition of sodium iodide or bromide to the solution for the hydrothermal synthesis, the peaks of O_{lat} were shifted by 0.3 eV and the peaks of O_{vac} were shifted by 0.5 eV towards high binding energies.

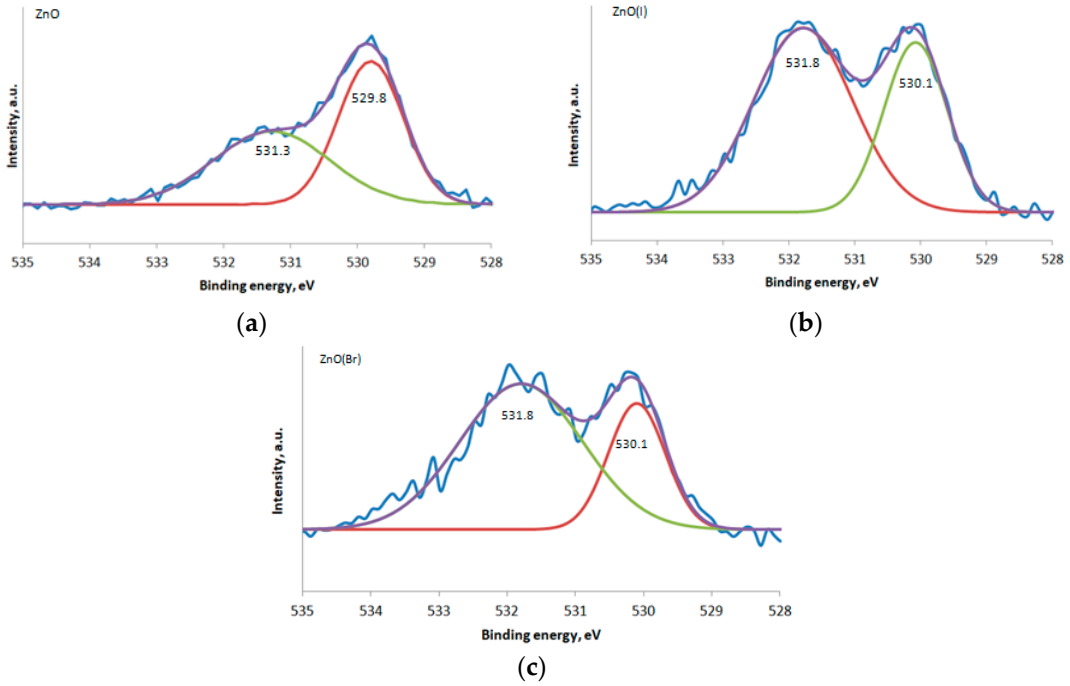

Figure 6. XPS spectra of O1s levels: (**a**)—ZnO, (**b**)—ZnO(I), (**c**)—ZnO(Br).

Table 1. Parameters of O1s spectra of zinc oxide nanowire samples.

Element		ZnO	ZnO(I)	ZnO(Br)
O_{lat}	Center, eV	529.8	530.1	530.1
	FWHM, eV	1.13	1.13	0.98
	Area, %	52	37	29
O_{vac}	Center, eV	531.3	531.8	531.8
	FWHM, eV	2.04	1.76	2.12
	Area, %	48	63	71

Iodine and bromine were not observed on the surfaces of the zinc oxide layers after the annealing at 350 °C in air (Figure 4). At the same time, there were significant changes in the spectra of the oxygen core levels after the sacrificial doping (Figure 6).

The study of the sensor properties showed that the sensitivity of the non-doped zinc oxide to the isopropyl alcohol vapors was 2.51, the sensitivity of the ZnO doped with iodine was 2.97, and the sensitivity of the ZnO doped with bromine was 4.03. The response and recovery times for each sample were calculated. The results are shown in Table 2. It was found that the response time of the doped samples decreased. The recovery time of the iodine-doped samples was reduced by almost two times and that of the bromine-doped samples was slightly increased in comparison with the pure zinc oxide nanowires.

Table 2. Sensor properties of zinc oxide nanowires samples.

Sample	Operating Temperature, °C	S (R_a/R_g)	Response Time, s	Recovery Time, s
ZnO	150	2.51	124	222
ZnO(I)		2.97	54	114
ZnO(Br)		4.03	76	272

Figure 7 shows a comparison between the time dependencies of the responses of the non-doped samples, with the bromine-doped samples having the highest sensitivity. Exposure to isopropyl alcohol vapors led to reversible changes in the resistance of the

gas-sensitive layers. The decrease in the resistance was due to the adsorption of isopropyl alcohol vapors on the surface of the nanowires, followed by redox reactions between the organic vapors and oxygen on the surface [25]. The electrons returned to the material volume, so the conductivity increased. The potential barriers between the zinc oxide nanowires were reduced.

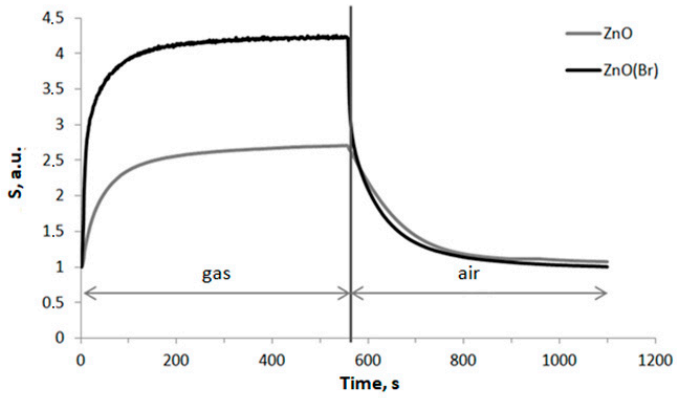

Figure 7. Time dependence of sensitivity of zinc oxide nanowire samples to isopropyl alcohol vapors.

4. Discussion

In the solution used for the hydrothermal synthesis of the zinc oxide nanowires, zinc nitrate was a source of Zn^{2+} ions and HMTA ensured the alkaline medium and OH^{-}ions during a slow decomposition. The occurring chemical reactions are described by the following equations:

$$C_6H_{12}N_4 + 6H_2O \rightarrow 6HCHO + 4NH_3,$$

$$NH_3 + H_2O \rightarrow NH_4^+ + OH^-,$$

$$2OH^- + Zn^{2+} \rightarrow Zn(OH)_2,$$

$$2Zn(OH)_2 \rightarrow [ZnO]_b + [ZnO]_s + 2H_2O,$$

$$[ZnO]_s + 2NaI + H_2O \rightarrow ZnI_2 + 2NaOH,$$

$$[ZnO]_s + 2NaBr + H_2O \rightarrow ZnBr_2 + 2NaOH.$$

In these equations, $[ZnO]_b$ is a zinc oxide molecule formed in the volume of the sensor layer and $[ZnO]_s$ is a zinc oxide molecule on the surface of the sensor layer.

The impact of the iodine on the reorganization of the surface composition can be explained by the model of modification of the subsurface structure of the ZnO described below. It is known that anionic and cationic sublattices exist in oxide nanocrystals. The iodine or bromine left the surface layer during the annealing. This was confirmed experimentally, since no iodine or bromine was observed on the surface of the doped ZnO nanowires in the XPS studies. Iodine could escape from the surface as I_2 or as ZnI_2, and bromine as Br_2 or $ZnBr_2$. The most significant change in the hydrophilic properties was caused by the removal of ZnI_2 or $ZnBr_2$ from the surface in a neutral form, which was accompanied by the appearance of vacancies (one in the zinc sublattice and two in the iodine or bromine sublattice). Thus, the localized negative iodine or bromine charges and a positively charged zinc vacancy should have remained in the crystal lattice. H_2O molecules could adsorb on the zinc vacancy. Along with this, a bond between a lone electron pair of an oxygen atom and a zinc vacancy was formed. A negative charge existed in the crystal

lattice; therefore, the probability of oxygen ionosorption increased. Thus, H_2O molecules and oxygen ions were adsorbed on the zinc oxide surface. A reaction between them could lead to the formation of negatively charged and neutral OH-groups.

For gas sensors, an important parameter is the specific surface area required for the adsorption of molecules. Due to the fact that not the entire surface of the material is used for sensing, an important criterion is the ratio of the surface to the volume. Nanostructures can significantly improve this parameter by playing the role of active layers. Therefore, nanostructures such as nanofibers and nanowires can significantly increase the active area and arouse interest among researchers [33]. Vacancies in the oxygen sublattice serve as adsorption sites, so their presence increases the reactivity of the surface. However, at the same time, gas sensors based on zinc oxide show a response to all gases. When a sensor is exposed to reducing gases, its resistance decreases, and when sensor is exposed to oxidizing gases, it increases. An effective way of ensuring selectivity is to design multisensors, the signal in which is measured from an array of sensors [33,34].

The reaction of the zinc oxide with the isopropyl alcohol (reducing gas) could be divided into two stages. At the first stage, oxygen molecules were adsorbed on the surface of the zinc oxide, with the subsequent filling of the oxygen vacancies. In this case, the electrons moved from the conduction band of the zinc oxide to the adsorbed oxygen, which resulted in an increase in resistance. Thus, oxygen vacancies stimulated the oxygen chemisorption. The higher the concentration of the oxygen vacancies, the more oxygen molecules were adsorbed, and more electrons left the conduction band of the oxide. At the second stage, when the sensor layer was placed in the atmosphere of an isopropyl alcohol vapor, an oxidizing–reducing reaction occurred. As a result, the electrons returned to the zinc oxide volume and the resistance decreased. The adsorbed oxygen molecules took part in the oxidation of isopropyl alcohol molecules, while oxygen vacancies reappeared in the zinc oxide lattice.

Another possible mechanism can be attributed to the reaction of the target gas molecules with the OH-groups adsorbed on the surface. At the same time, hydroxyl groups can perform several functions. Firstly, they can oxidize the desorbed gas molecules at low temperatures, as shown in [35]. Hydroxyl groups can also be the adsorption sites of target gas molecules [25]. The scheme of interaction between the isopropyl alcohol molecules, the surface of the zinc oxide, and the hydroxyl groups is shown in Figure 8.

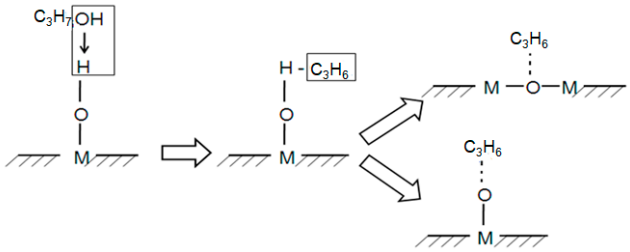

Figure 8. Scheme of isopropyl alcohol molecules and OH-groups interaction on the surface of metal oxide.

The developed principles for the energy management of the adsorption sites are of interest for the development of percolation-type sensors with additional areas for water vapor traps [23]. An example of such a structure is shown in Figure 9.

In such sensors, a percolation element is located between the electrodes. A current flows through this element, which changes as a result of the reactions of the surface of the nanowires with the target gas molecules. On the sides of the percolation element, there are free-standing nanowires that do not have electrical contact with the electrodes. The design of the surface defect structure and the formation of additional oxygen vacancies provide the control of the hydrophilic properties of free-standing nanowires. This makes it possible to capture water vapors from the atmosphere. Thus, such a design is promising for enhancing the stability of gas sensors in a high humidity.

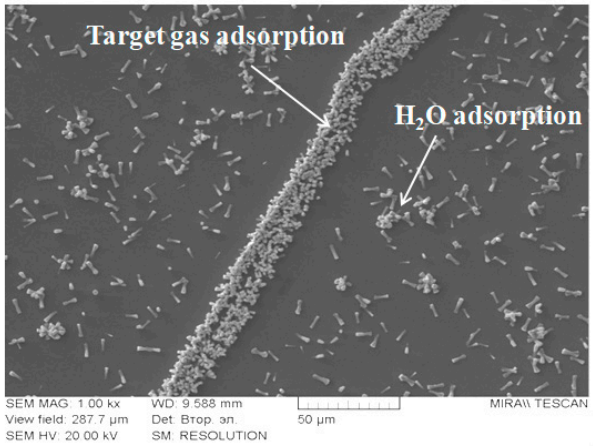

Figure 9. SEM image of gas-sensitive layer of percolation type with adsorption sites for water molecules. Adapted with permission from Ref. [23]. 2023, Springer Nature.

5. Conclusions

The analysis of the surface composition of the zinc oxide nanowires showed that, as a result of sacrificial doping with iodine and bromine, a considerable redistribution of the electron density and an increase in the concentration of the oxygen vacancies/hydroxyl groups was observed. A model for the reorganization of the surface bonds with iodine removal during the annealing was proposed. The influence of the oxygen vacancies in the zinc oxide on the chemisorption processes was analyzed. Experimental methods for increasing sensitivity were proposed. It was found that the ZnO layers modified with iodine and bromine had a higher gas sensitivity. This was due to the formation of additional oxygen vacancies or hydroxyl groups, which were sites for the adsorption of negatively charged oxygen ions participating in the reactions of reducing gas oxidation. The developed methods for controlling the surface properties, in particular the hydrophilic properties, are of interest for percolation sensors containing additional water vapor adsorption sites. Thus, this is one of the possible ways ofincreasing the stability of sensor characteristics in a humid atmosphere.

Author Contributions: Conceptualization, V.M. and S.N.; investigation, A.B., Z.S. and S.N.; resources, Z.S. and S.N.; writing—original draft preparation, S.N.; writing—review and editing, V.M., Z.S. and A.B.; visualization, A.B.; supervision, V.M.; project administration, S.N. All authors have read and agreed to the published version of the manuscript.

Funding: This research received no external funding.

Data Availability Statement: Raw experimental data are available from the authors on demand.

Conflicts of Interest: The authors declare no conflict of interest.

References

1. Armitage, B.I.; Murugappan, K.; Lefferts, M.J.; Cowsik, A.; Castell, M.R. Conducting polymer percolation gas sensor on a flexible substrate. *J. Mater. Chem. C* **2020**, *8*, 12669. [CrossRef]
2. Staerz, A.; Weimar, U.; Barsan, N. Current state of knowledge on the metal oxide based gas sensing mechanism. *Sens. Act. B* **2022**, *358*, 13153. [CrossRef]
3. Goel, N.; Kunal, K.; Kushwaha, A.; Kuma, M. Metal oxide semiconductors for gas sensing. *Eng. Rep.* **2022**, e12604. [CrossRef]
4. Bobkov, A.; Luchinin, V.; Moshnikov, V.; Nalimova, S.; Spivak, Y. Impedance spectroscopy of hierarchical porous nanomaterials based on por-Si, por-Si incorporated by Ni and metal oxides for gas sensors. *Sensors* **2022**, *22*, 1530. [CrossRef] [PubMed]
5. Choi, M.S.; Na, H.G.; Mirzaei, A.; Bang, J.H.; Oum, W.; Han, S.; Choi, S.-W.; Kim, M.; Jin, C.; Kim, S.S.; et al. Room-temperature NO_2 sensor based on electrochemically etched porous silicon. *J. Alloys Compd.* **2019**, *811*, 151975. [CrossRef]
6. Zhang, D.; Yang, Z.; Yu, S.; Mi, Q.; Pan, Q. Diversiform metal oxide-based hybrid nanostructures for gas sensing with versatile prospects. *Coord. Chem. Rev.* **2020**, *413*, 213272. [CrossRef]
7. Gautam, Y.K.; Sharma, K.; Tyagi, S.; Ambedkar, A.K.; Chaudhary, M.; Pal Singh, B. Nanostructured metal oxide semiconductor-based sensors for greenhouse gas detection: Progress and challenges. *R. Soc. Open Sci.* **2021**, *8*, 201324. [CrossRef]

8. Maccato, C.; Barreca, D. *Tailored Functional Oxide Nanomaterials: From Design to Multi-Purpose Applications*; Wiley: Weinheim, Germany, 2022; ISBN 978-3-527-34759-9.
9. Maziarz, W. TiO_2/SnO_2 and TiO_2/CuO thin film nano-heterostructures as gas sensors. *Appl. Surf. Sci.* **2019**, *480*, 361–370. [CrossRef]
10. Zhou, X.; Wang, A.; Wang, Y.; Bian, L.; Yang, Z.; Bian, Y.; Gong, Y.; Wu, X.; Han, N.; Chen, Y. Crystal-Defect-Dependent Gas-Sensing Mechanism of the Single ZnO Nanowire Sensors. *ACS Sens.* **2018**, *3*, 2385–2393. [CrossRef]
11. Pronin, I.A.; Yakushova, N.D.; Averin, I.A.; Karmanov, A.A.; Komolov, A.S.; Sychev, M.M.; Moshnikov, V.A.; Terukov, E.I. Chemical binding of carbon dioxide on zinc oxide powders prepared by mechanical milling. *Inorg. Mater.* **2021**, *57*, 1140–1144. [CrossRef]
12. Marikutsa, A.; Rumyantseva, M.; Gaskov, A.; Batuk, M.; Hadermann, J.; Sarmadian, N.; Saniz, R.; Partoens, B.; Lamoen, D. Effect of Zinc Oxide Modification by Indium Oxide on Microstructure, Adsorbed Surface Species, and Sensitivity to CO. *Front. Mater.* **2019**, *6*, 43. [CrossRef]
13. Krasteva, L.K.; Dimitrov, D.T.; Papazova, K.I.; Nikolaev, N.K.; Peshkova, T.V.; Kaneva, N.V.; Moshnikov, V.A.; Gracheva, I.E.; Karpova, S.S. Synthesis and characterization of nanostructured zinc oxide layers for sensor applications. *Semiconductors* **2013**, *47*, 586–591. [CrossRef]
14. Ryabko, A.A.; Bobkov, A.A.; Nalimova, S.S.; Maksimov, A.I.; Levitskii, V.S.; Moshnikov, V.A.; Terukov, E.I. Gas sensitivity of nanostructured coatings based on zinc oxide nanorods under combined activation. *Tech. Phys.* **2022**, *92*, 644–649. [CrossRef]
15. Kang, Y.; Yu, F.; Zhang, L.; Wang, W.; Chen, L.; Li, Y. Review of ZnO-based nanomaterials in gas sensors. *Solid State Ion.* **2021**, *360*, 115544. [CrossRef]
16. Wang, C.-N.; Li, Y.-L.; Gong, F.-L.; Zhang, Y.-H.; Fang, S.-M.; Zhang, H.-L. Advances in doped ZnO nanostructures for gas sensor. *Chem. Rec.* **2020**, *20*, 1–16. [CrossRef] [PubMed]
17. Shooshtari, M.; Pahlavan, S.; Rahbarpour, S.; Ghafoorifard, H. Investigating Organic Vapor Sensing Properties of Composite Carbon Nanotube-Zinc Oxide Nanowire. *Chemosensors* **2022**, *10*, 205. [CrossRef]
18. Han, N.; Wu, X.; Chai, L.; Liu, H.; Chen, Y. Counterintuitive sensing mechanism of ZnO nanoparticle based gas sensors. *Sens. Act. B* **2010**, *150*, 230–238. [CrossRef]
19. Ahn, M.-W.; Park, K.-S.; Heo, J.-H.; Park, J.-G.; Kim, D.-W.; Choi, K.J.; Lee, J.-H.; Hong, S.-H. Gas sensing properties of defect-controlled ZnO-nanowire gas sensor. *Appl. Phys. Lett.* **2008**, *93*, 263103. [CrossRef]
20. Zeng, Q.; Cui, Y.; Zhu, L.; Yao, Y. Increasing oxygen vacancies at room temperature in SnO_2 for enhancing ethanol gas sensing. *Mater. Sci. Semicond. Proc.* **2020**, *111*, 104962. [CrossRef]
21. Yu, W.; Shen, Z.; Peng, F.; Lu, Y.; Ged, M.; Fu, X.; Sun, Y.; Chen, X.; Dai, N. Improving gas sensing performance by oxygen vacancies in sub-stoichiometric WO_{3-x}. *RSC Adv.* **2019**, *9*, 7723–7728. [CrossRef]
22. Wang, J.; Chen, R.; Xiang, L.; Komarneni, S. Synthesis, properties and applications of ZnO nanomaterials with oxygen vacancies: A review. *Ceram. Int.* **2018**, *44*, 7357–7377. [CrossRef]
23. Bobkov, A.A.; Pronin, I.A.; Moshnikov, V.A.; Yakushova, N.D.; Karmanov, A.A.; Averin, I.A.; Somov, P.A.; Terukov, E.I. Creating lithographic pictures using faceted zinc oxide microparticles on a silicon substrate. *Tech. Phys. Lett.* **2018**, *44*, 694–696. [CrossRef]
24. Hsieh, P.-T.; Chen, Y.-C.; Kao, K.-S.; Wang, C.-M. Luminescence mechanism of ZnO thin film investigated by XPS measurement. *Appl. Phys. A* **2008**, *90*, 317–321. [CrossRef]
25. Karpova, S.S.; Moshnikov, V.A.; Maksimov, A.I.; Mjakin, S.V.; Kazantseva, N.E. Study of the effect of the acid-base surface properties of ZnO, Fe_2O_3 and $ZnFe_2O_4$ oxides on their gas sensitivity to ethanol vapor. *Semiconductors* **2013**, *47*, 1026–1030. [CrossRef]
26. Nalimova, S.S.; Shomakhov, Z.V.; Moshnikov, V.A.; Bobkov, A.A.; Ryabko, A.A.; Kalazhokov, Z.K. An X-ray photoelectron spectroscopy study of zinc stannate layer formation. *Tech. Phys.* **2020**, *65*, 1087–1090. [CrossRef]
27. Shomakhov, Z.V.; Nalimova, S.S.; Kalazhokov, Z.K.; Moshnikov, V.A. Analysis of surface composition changes in the formation of zinc stannate nanostructures. *Phys.-Chem. Asp. Study Clust. Nanostruct. Nanomater.* **2020**, *12*, 222–231. [CrossRef]
28. Fouad, O.A.; Ismail, A.A.; Zaki, Z.I.; Mohamed, R.M. Zinc oxide thin films prepared by thermal evaporation deposition and its photocatalytic activity. *Appl. Catal. B* **2006**, *62*, 144–149. [CrossRef]
29. Gancheva, M.; Markova-Velichkova, M.; Atanasova, G.; Kovacheva, D.; Uzunov, I.; Cukeva, R. Design and photocatalytic activity of nanosized zinc oxides. *Appl. Surf. Sci.* **2016**, *368*, 258–266. [CrossRef]
30. Ikeo, N.; Iijima, Y.; Nimura, N.; Sigematsu, M.; Tazawa, T.; Matsumoto, S.; Kojima, K.; Nagasawa, Y. *Handbook of X-ray Photoelectron Spectroscopy*; JEOL: Akishima, Japan, 1991.
31. Liu, S.; Li, G.; Xiao, L.; Jia, B.; Gao, Y.; Wang, Q. Effect of morphology evolution on the thermoelectric properties of oxidized ZnO thin films. *Appl. Surf. Sci.* **2018**, *436*, 354–361. [CrossRef]
32. Abdullin, K.A.; Gabdullin, M.T.; Zhumagulov, S.K.; Ismailova, G.A.; Gritsenko, L.V.; Kedruk, Y.Y.; Mirzaeian, M. Stabilization of the Surface of ZnO Films and Elimination of the Aging Effect. *Materials* **2021**, *14*, 6535. [CrossRef]
33. Bobkov, A.; Varezhnikov, A.; Plugin, I.; Fedorov, F.S.; Goffman, V.; Moshnikov, V.; Sysoev, V.; Trouillet, V.; Geckle, U.; Sommer, M. The multisensor array based on grown-on-chip zinc oxide nanorod network for selective discrimination of alcohol vapors at sub-ppm range. *Sensors* **2019**, *19*, 4265. [CrossRef] [PubMed]

34. Fedorov, F.; Vasilkov, M.; Lashkov, A.; Varezhnikov, A.; Fuchs, D.; Kübel, C.; Bruns, M.; Sommer, M.; Sysoev, V. Toward new gas-analytical multisensor chips based on titanium oxide nanotube array. *Sci. Rep.* **2017**, *7*, 9732. [CrossRef] [PubMed]
35. Kutukov, P.; Rumyantseva, M.; Krivetskiy, V.; Filatova, D.; Batuk, M.; Hadermann, J.; Khmelevsky, N.; Aksenenko, A.; Gaskov, A. Influence of Mono- and Bimetallic PtO_x, PdO_x, $PtPdO_x$ Clusters on CO Sensing by SnO_2 Based Gas Sensors. *Nanomaterials* **2018**, *8*, 917. [CrossRef] [PubMed]